**Under review at Surgical and Radiologic Anatomy (Springer Nature)**

# Variability in peroneus brevis tendon localisation on magnetic resonance at the lateral malleolus: an observational cohort study

Rafał Zych[1], Dawid Dziedzic[1], Katarzyna Bokwa-Dąbrowska[2,3], Dan Mocanu[3], Pawel Szaro[1,2,3]

1. Department of Clinical and Descriptive Anatomy, Medical University of Warsaw, Poland
2. Department of Radiology, Institute of Clinical Sciences, Sahlgrenska Academy, University of Gothenburg, Gothenburg, Sweden.
3. Department of Musculoskeletal Radiology, Sahlgrenska University Hospital, Gothenburg, Sweden

## Abstract

### Purpose

This study aimed to classify anatomical variants in peroneus brevis localisation and assess associations with tendon shape, size, and the presence of the peroneus quartus muscle and low-lying peroneus brevis muscle.

### Methods

This observational cohort study included 230 ankle magnetic resonance examinations (3T) with normal peroneal tendons. Peroneus brevis localisation relative to peroneus longus was categorised into four types: medial, overlapping with medial protrusion, overlapping with

lateral protrusion, and overlapping with both. Tendon shape was classified as general flat, flattened convex medially, flattened convex laterally, or oval. Associations between localisation and shape were tested using chi-square. Differences in cross-sectional area ($mm^2$) and width (mm) across groups were assessed with analysis of variance and Tukey's post hoc test. A regression model identified predictors of tendon overlap.

**Results**

The most common localisation was overlap with medial protrusion (72.0%), followed by medial, lateral, and combined protrusions. Localisation was significantly associated with shape ($p < 0.001$); oval tendons were typically medial, while flattened tendons overlapped. Width and cross-sectional area differed significantly across positions ($p = 0.0088$), with the largest area in tendons protruding medially and laterally (16.9 $mm^2$). Width correlated strongly with overlap ($r = 0.79$, $p < 0.001$) and was the strongest predictor in regression ($\beta = 0.51$, $p < 0.001$). Peroneus quartus was independently associated with increased overlap ($\beta = 0.22$, $p = 0.03$), while low-lying peroneus brevis muscle showed no significant effect.

**Conclusion**

Peroneus brevis localisation is highly variable and depends on its shape, width, and the presence of peroneus quartus.

## Background and rationale

Ankle injuries are common and often complex, involving ligaments, cartilage, bone, or tendons injury. A frequent clinical challenge is the persistence of symptoms after ankle sprain, which can be caused by underdiagnosed peroneal tendon injuries [10]. Peroneal tendon instability and split ruptures are both clinically and radiologically significant, yet they are frequently missed, with estimates suggesting that up to half of the cases go undiagnosed [1, 2]. The true incidence of peroneus brevis split tears is unknown; however, some studies report a prevalence as high as 30%–60% [12, 19].

The peroneus brevis tendon courses along the posterior surface of the lateral malleolus, gliding in the malleolar groove in direct relation to the peroneus longus tendon. Both tendons are stabilised posteriorly by the superior peroneal retinaculum, forming the superior peroneal tunnel [1]. Their close anatomical relationship in this narrow space is particularly relevant, as longitudinal tendon splits most commonly occur [2, 11, 28].

The distal attachment of the fibularis brevis tendon is known to demonstrate considerable morphological variability, with multiple cadaveric studies proposing detailed classification systems based on anatomical dissection [13, 14, 16]. Most of these studies have concentrated on variations in the number and configuration of distal tendon bands and their relationship to structures such as the fibularis digiti quinti. Classifications of the peroneus brevis insertion have been proposed in adults and foetuses, identifying types with single, bifurcated, or even triple distal attachments, and highlighting clinically relevant subtypes based on insertion points on the fifth metatarsal or adjacent fascia [13, 14, 29]. Beyond distal anatomy, research has also explored the relationship between the location of the musculotendinous junction and the risk of tendon injury. A cadaveric study found that a low-lying peroneus brevis muscle belly was statistically associated with longitudinal split tears of the fibularis brevis [6].

Other anatomical variations related to peroneus brevis tears include the shape and depth of the fibular groove, presence of accessory muscles like the peroneus quartus, a low-lying muscle belly of the peroneus brevis, and hypertrophy of the peroneal tubercle [3, 11, 19, 20, 25, 26, 28]. Some authors have suggested a possible relationship between split rupture and the shape of the peroneus brevis [9]. Peroneus brevis split tears are more common [3, 18] than peroneus longus tears and typically occur at the level of the lateral malleolus[7, 23]. Peroneal tendon pathology is frequently linked with chronic lateral ankle instability. Peroneal tendon tears are associated with ankle instability and hindfoot varus [21].

Dynamic studies have demonstrated that during dorsiflexion, the peroneus brevis may be compressed against the fibula by the overlying peroneus longus, a mechanism thought to contribute to longitudinal tears [17]. However, these findings are based on small sample sizes (22 and 39 participants, respectively).

Despite previous cadaveric studies [6, 12-14] and a growing appreciation for the role of anatomical variation in tendon pathology, the in vivo spatial relationship between the peroneus brevis and peroneus longus tendons along their retromalleolar course remains poorly understood.

Our study addresses this gap by investigating the anatomical variants in the localisation of the peroneus brevis tendon relative to the peroneus longus in vivo on magnetic resonance imaging. We also explore potential factors that may influence this localisation, including tendon shape, cross-sectional area, presence of peroneus quartus, and demographic characteristics. By analysing a cohort of asymptomatic individuals using high-resolution

imaging, we aim to improve the understanding of normal anatomical variability and its potential relevance to peroneal tendon biomechanics and pathology.

## Objectives

To assess anatomical variations in the relative positioning of the peroneus brevis and peroneus longus tendons at the level of the lateral malleolus using in vivo magnetic resonance imaging. The study also explored factors that may influence these positional variations.

*Research questions:*

1. What are the most common anatomical variants in the relative localisation of the peroneus brevis tendon to the peroneus longus?
2. Are shape, cross-sectional area, the presence of peroneus quartus, and low-lying muscle belly related to the position of peroneus brevis?

## Methods

### 1. Study design

This is an observational cohort study. The study was conducted and reported according to the Strengthening the Reporting of Observational Studies in Epidemiology (STROBE) guidelines for observational studies [27].

### 2. Setting

We re-evaluated ankle MRI examinations performed on a 3T scanner between 2019 and 2024 at our institution using standard protocol.

## 3. Participants

Inclusion criteria were normal peroneal tendons and normal superior peroneal retinaculum. Exclusion criteria included higher signal of peroneus brevis or longus on proton density weighted or T2-weighted images, tenosynovitis in the peroneal synovial sheath and bone marrow oedema, lateral malleolar fracture and symptoms in relation to lateral malleolus in the referral letter, history of peroneus tendon pathology, prior surgery, inflammatory conditions, or tumours.

## 4. Outcomes

**The primary outcome** is the relative localisation of the peroneus brevis tendon in relation to the peroneus longus tendon at the level of the lateral malleolus, assessed on axial magnetic resonance imaging. Localisation was categorised as:

a) peroneus brevis overlaps the peroneus longus and protrudes medially;

b) peroneus brevis is positioned entirely medial to the peroneus longus;

c) peroneus brevis overlaps the peroneus longus and protrudes laterally; and

d) peroneus brevis overlaps the peroneus longus and protrudes both medially and laterally.

**Secondary outcomes** are shape, cross-sectional area of the peroneus brevis tendon and presence of the peroneus quartus muscle.

The shape of the peroneus brevis tendon classified into four types based on cross-sectional morphology:

a) general flat

b) flattened with lateral convexity

c) flattened with medial convexity

d) oval

Cross-sectional area of the peroneus brevis tendon (in $mm^2$), measured on axial images.

**Potential confounders**: age, sex, and side of the body (left or right ankle).

## 5. Data sources and measurements

MRI transverse sections (proton density-weighted) 1 cm above the lateral malleolus apex were identified by two independent musculoskeletal radiologists. Discrepancies were resolved by consensus. The sections were segmented using ImageJ, where the outlines of the peroneus brevis, peroneus longus, and fibula were segmented by two raters (musculoskeletal radiologist with 10 years' experience and physiotherapist after getting a training session from musculoskeletal radiologist) to obtain coordinates (X, Y) allowing to asses the cross-sectional areas of the tendons (mm2) and overlap (mm).

## 6. Sample size

A sample size of 230 patients was selected based on our preliminary study to achieve the power for the chi-square test (as the main analysis) of more than 0.8. The effect size, measured using Cramér's V, was 0.38.

## 7. Quantitative analysis

Tendon area (in $mm^2$) as a continuous variable was compared between four tendon shapes using analysis of variance (ANOVA).

## 8. Statistical analysis

Inter-rater agreement was assessed using Cohen's kappa for categorical variables (localization and shape), and the intraclass correlation coefficient (ICC(2,1)) for continuous measurements (cross-sectional area).

Chi-square tests were used to assess the association between the relative position of the peroneus brevis tendon and its shape, as well as between age groups (18–30 years, 31–60 years, and older than 61 years) and peroneus brevis shape. In case of a significant chi-square result, Tukey's HSD post hoc test was applied to identify specific group differences.

ANOVA was used to evaluate if cross-sectional area of the peroneus brevis tendon differed between different shape and localisations. The assumption of normality was evaluated using the Shapiro–Wilk test, and homogeneity of variance was assessed with Levene's test. A significance level of $p < 0.05$ was considered significant. Post-hoc comparisons were conducted using Tukey's honest significant difference (HSD) test.

The distribution of overlap values was non-normal in at least two groups (Shapiro–Wilk $p < 0.001$) and Levene's test indicated significant heterogeneity of variances ($p = 0.0037$). Therefore, we used the Kruskal–Wallis test followed by pairwise Wilcoxon tests with Benjamini–Hochberg correction.

We used a multiple linear regression model to assess association between variables and the degree of tendon overlap (mm). The regression model was constructed using four predictors: presence of a peroneus quartus muscle, presence of a low-lying peroneus brevis muscle belly, cross-sectional area of the peroneus longus tendon, and width of the peroneus brevis tendon. Given evidence of non-constant variance (Breusch–Pagan test, $p < 0.001$), robust standard errors (HC1 estimator) were applied to all coefficient estimates. Model assumptions were

evaluated through residual plots and normality testing (Shapiro–Wilk, p = 0.026). Model robustness was assessed by influence diagnostics and sensitivity analysis excluding the most influential observation (one case).

## Results

### 1. Study population

We re-evaluated 569 MRI examinations. Exclusion criteria were fractures (49), ligament injuries, pathological changes in the peroneal tendons, lateral malleolar symptoms (147), history of peroneus tendon pathology or post-operative changes in lateral ligaments or peroneal tendons (129), infections (8), or ganglion cysts (6). A total of 230 consecutive MRI examinations met the inclusion criteria.

The mean age was 41.9 years (range: 12–72 years), with a standard deviation of 14.9 years. Among the total of 230 patients, there were 121 males (52.6%) and 109 females (47.4%). The distribution of side was equal, with 115 patients on the left side (50.0%) and 115 patients on the right side (50.0%).

## 2. Outcome data and main results

### 2.1. Inter-rater agreement

Inter-rater agreement for the localization, shape, and cross-sectional area of the peroneus brevis tendon was almost perfect, according to the criteria by Landis and Koch [8]. Cohen's kappa was 0.85 (95% CI: 0.76–0.94) for localization and 0.87 (95% CI: 0.81–0.98) for shape. The intraclass correlation coefficient (ICC(2,1)) for cross-sectional area was 0.98 (95% CI:

0.97–0.99). Agreement for identifying a low-lying muscle belly (LLMB) was also almost perfect (kappa = 0.83, 95% CI: 0.73–0.92), while agreement for the presence of a peroneus quartus was moderate (kappa = 0.66, 95% CI: 0.54–0.78) [8]. Final ratings for localization, shape, LLMB, and peroneus quartus were based on consensus; for cross-sectional area, the mean value was used due to high agreement.

## 2.2. Variants in the position of the peroneus brevis tendon

The most common relative position was peroneus brevis overlaps peroneus longus and protrudes medially, observed in 161 cases (72.0%). The second most frequent position was peroneus brevis medial to peroneus longus, seen in 33 cases (15.1%), followed by peroneus brevis overlaps peroneus longus and protrudes laterally, observed in 22 cases (9.6%). The least common position was peroneus brevis overlaps peroneus longus and protrudes both laterally and medially, noted in 14 cases (6.0%) (Figure 1). The peroneus brevis tendon position was not significantly influenced by age, sex, or side ($p > 0.05$).

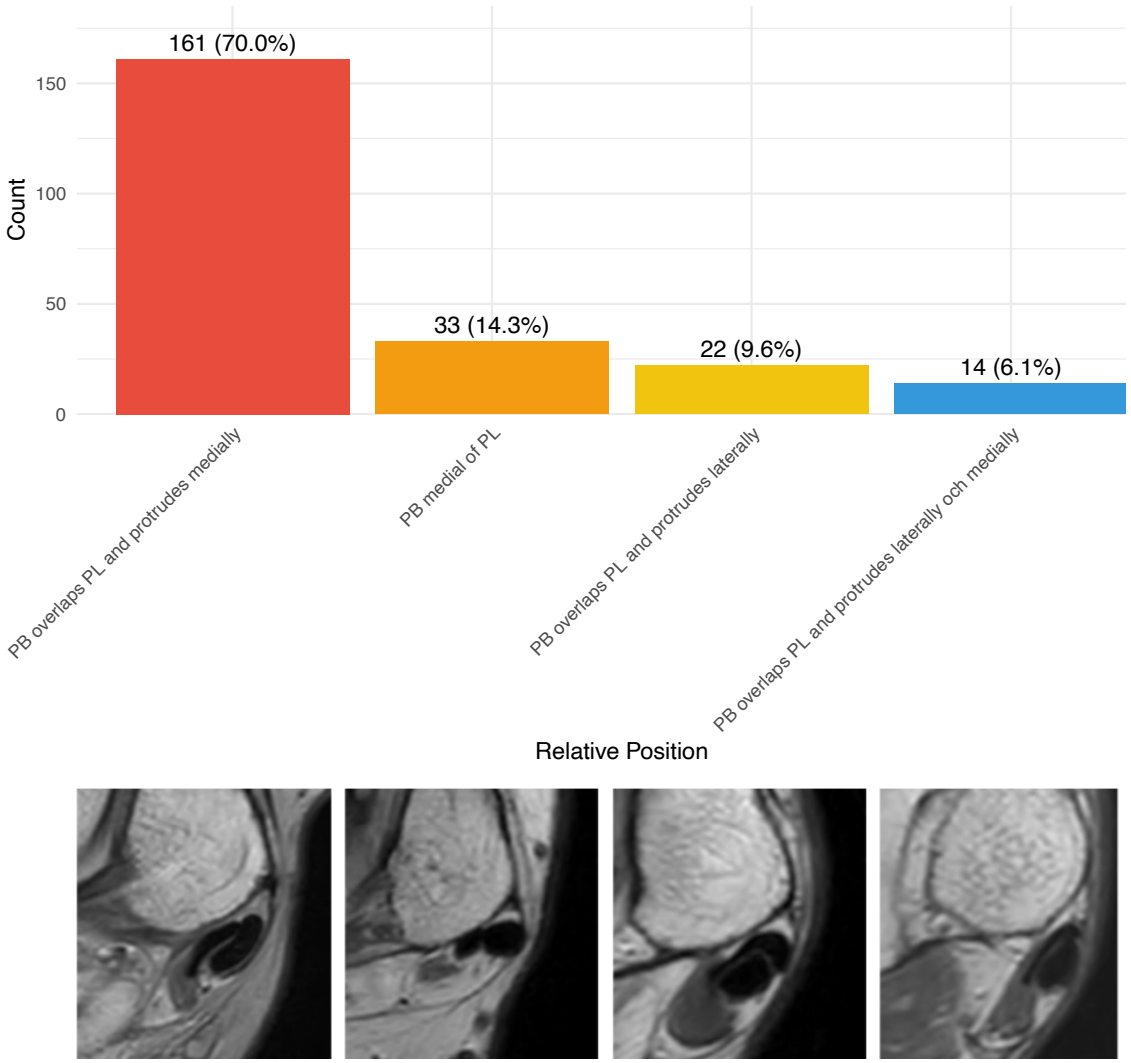


**Figure 1.** Bar chart illustrating the distribution of relative tendon positions with counts (n) and percentages (%). Examples from the magnetic resonance imaging (MRI), proton density-weighted images, transverse sections showing peroneal tendons in relation to lateral malleolus, left ankles. MRI sections below correspond to the bar chart above, with the same order and legend for tendon position. PB – peroneus brevis, PL – peroneus longus.

## 2.3. Tendon shape vs. localisation

The most frequent shape across all positions was general flat (82 cases, 36.3%), followed by flattened convex medially (81 cases, 35.8%), oval (42 cases, 18.3%), and flattened convex laterally (25 cases, 9.6%) (Figures 2 and 3).

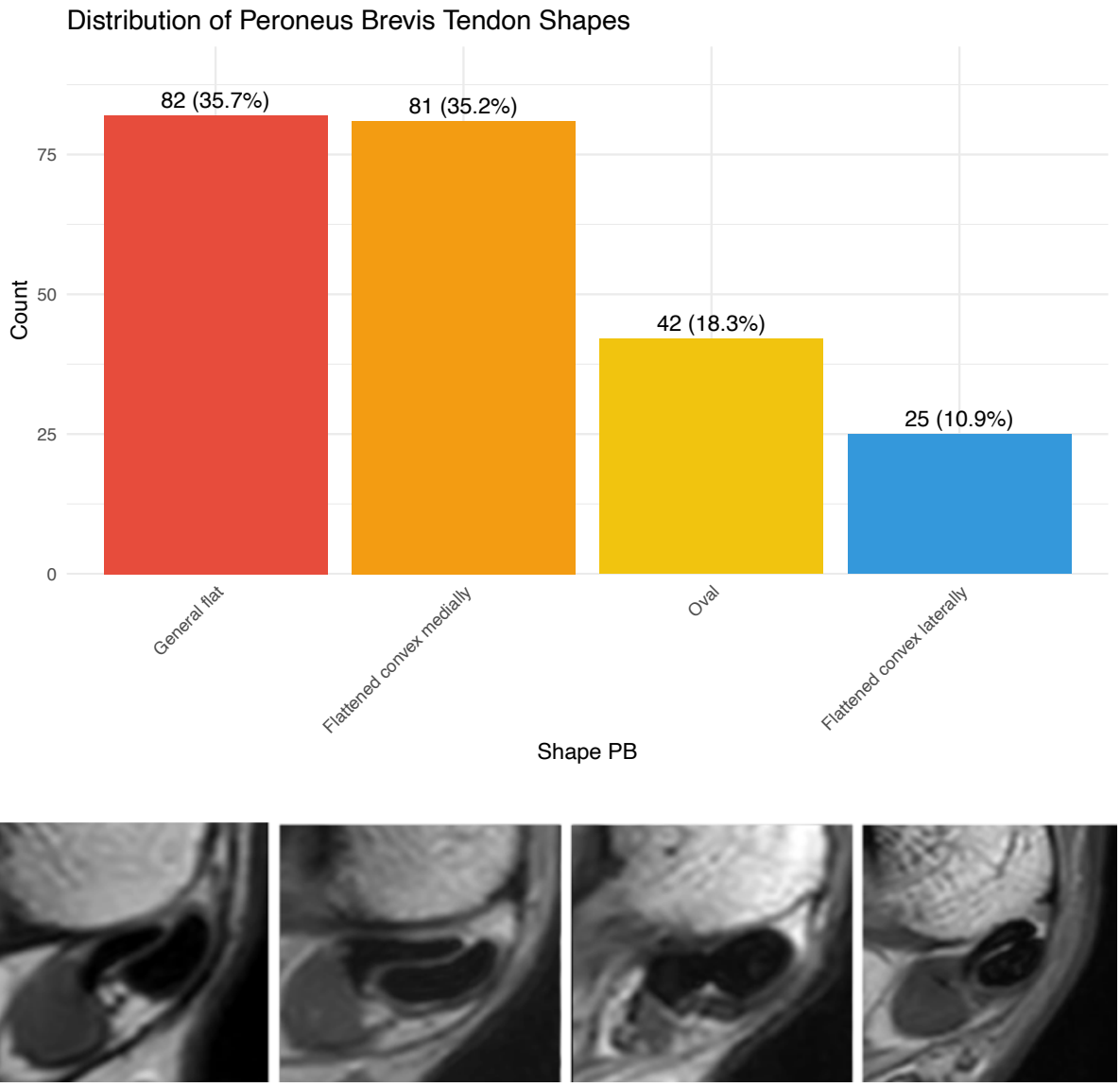


**Figure 2.** Bar chart showing the distribution of tendon shapes with examples from proton density weighted images. Examples from the magnetic resonance imaging (MRI), proton

density-weighted images, transverse sections showing peroneal tendons in relation to lateral malleolus, left ankles. MRI sections below correspond to the bar chart above, with the same order and legend for tendon position. PB – peroneus brevis.

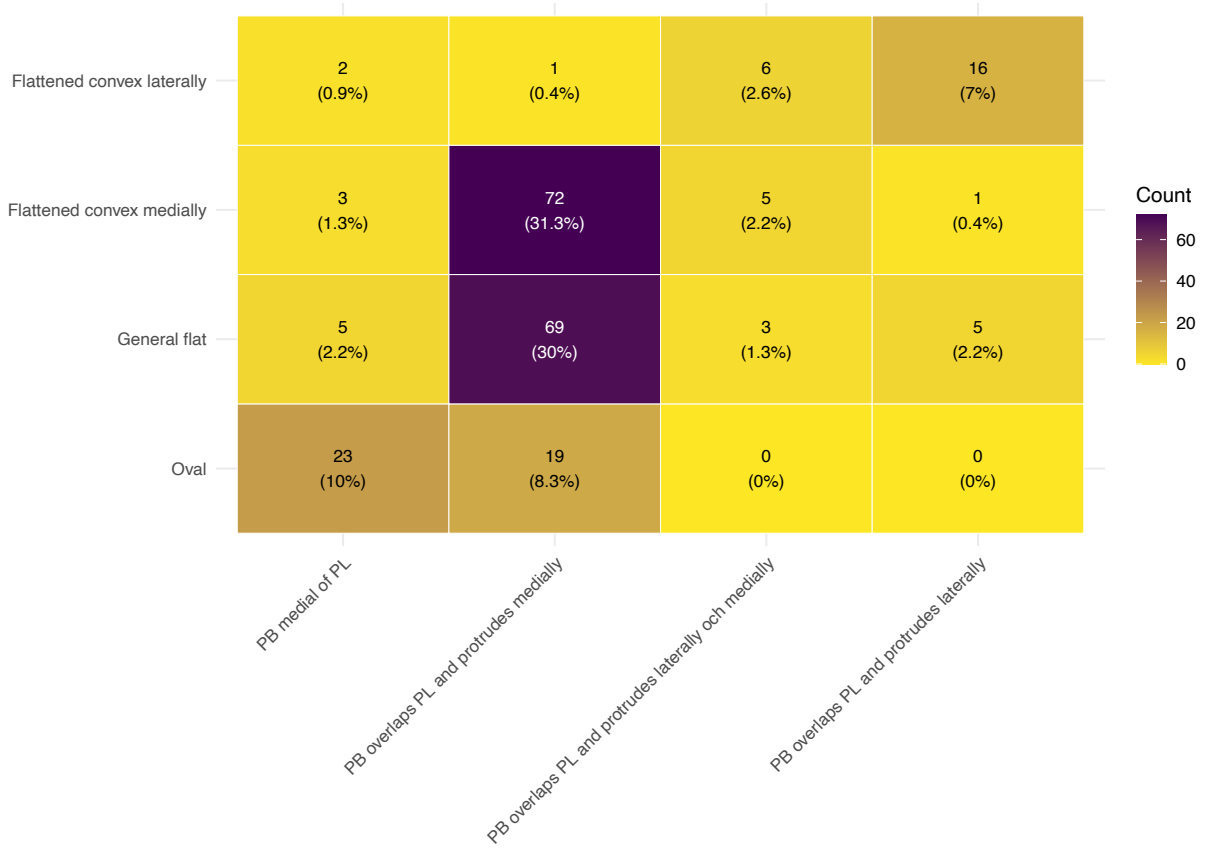


**Figure 3.** Distribution of peroneus brevis shape by localisation, transition matrix.

There was a significant association between the relative localisation of the peroneus brevis tendon and its cross-sectional shape (chi2 $\chi^2 = 189.41$, df = 9, $p < 0.001$). Peroneus brevis located medial to the peroneus longus were most commonly oval-shaped, while those overlapping and protruding medially were frequently flattened convex medially or general flat

(Figures 3 and 4). These findings suggest a morphological relationship between peroneus brevis shape and anatomical position.

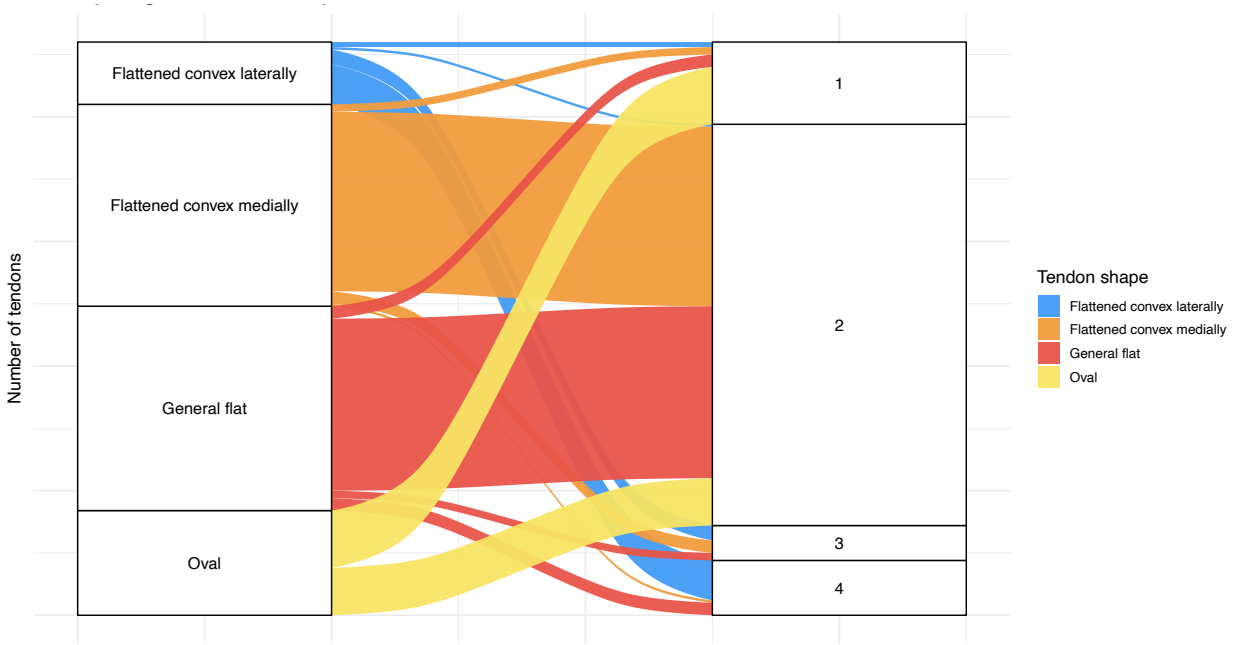


**Figure 4.** Sankey diagram illustrating the distribution of tendon shapes in relation to their localisation (1–4). The width of each flow is proportional to the number of tendons in each combination. On the left, the shape of the peroneus brevis tendon is shown, categorised as flattened convex laterally (blue), flattened convex medially (orange), general flat (red), or oval (yellow). These shapes are mapped to the tendon's relative localisation to the peroneus longus on the right side of the plot. 1 – peroneus brevis medial to peroneus longus, 2 – peroneus brevis overlaps peroneus longus and protrudes medially, 3 – peroneus brevis overlaps peroneus longus and protrudes both laterally and medially, and 4 – peroneus brevis overlaps peroneus longus and protrudes laterally

## 2.4. Tendon shape vs age group

The 'flattened convex medially' shape was most common in individuals aged 31–60 years (31.7%), while the 'flattened convex laterally' shape appeared more frequently in those over 61 years (38.9%). A Chi-square test confirmed a significant association between age group and peroneus brevis shape ($\chi^2 = 11.03$, df = 9, p = 0.004). Post-hoc analysis (Tukey's HSD) indicated that this difference was driven by comparisons between the 31–60 and 61+ age groups (mean difference = 2.24, p = 0.036) (Figure 5).

.

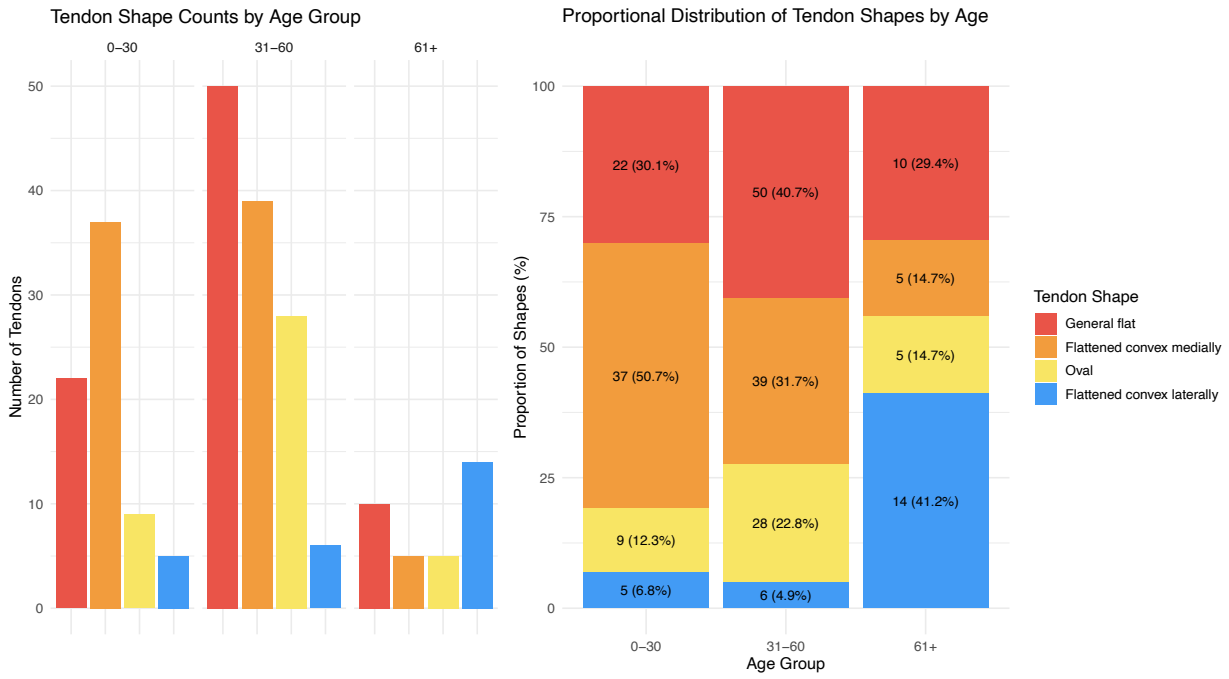


**Figure 5.** Combined visualisation of peroneus brevis tendon shape distribution across age groups. (Left) Absolute counts of each shape within age groups. (Right) Proportional distribution, highlighting shape frequency normalised to group size. Colour-coding

corresponds to tendon shape: general flat (red), flattened convex medially (orange), oval (yellow), and flattened convex laterally (blue).

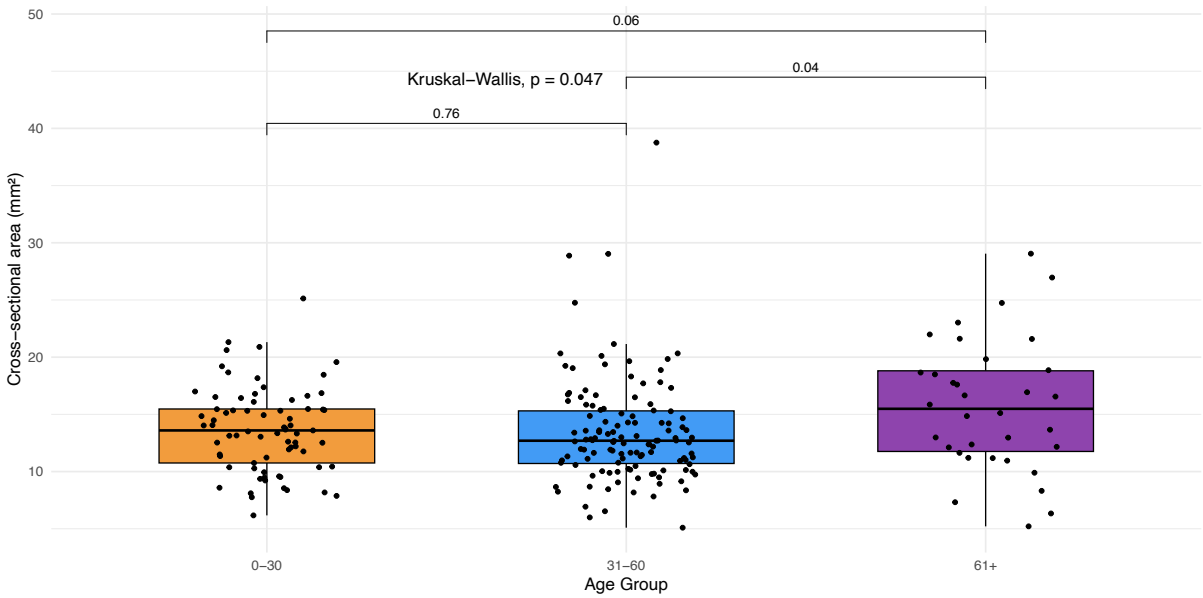


**Figure 6.** Peroneus brevis cross sectional area by age group. Boxplot showing the distribution of peroneus brevis tendon cross-sectional area (mm²) across age groups. Coloured boxes represent age categories: 0–30 (orange), 31–60 (blue), and 61+ (purple). Black dots indicate individual measurements. A Kruskal–Wallis test revealed a significant overall difference between groups, with pairwise comparisons indicating a significant difference between individuals aged 31–60 and those over 61 ($p = 0.036$).

## 2.5. Relation between tendon localisation and cross-sectional area

The mean peroneus brevis cross-sectional area (mm²) varied across different tendon positions (Table 1). The highest cross section area of the peroneus brevis was seen when it overlaps peroneus longus and protrudes laterally and medially (mean area of 16.9 mm², SD = 5.7).

**Table 1.** Differences in the cross-sectional area of peroneus brevis vs different positions of the peroneus brevis tendon.

| Relative Position | Count | Mean | SD | Min | Q1 | Median | Q3 | Max |
|---|---|---|---|---|---|---|---|---|
| PB medial of PL | 33 | 12.2 | 3.7 | 5.1 | 10.2 | 11.2 | 13.5 | 25.1 |
| PB overlaps PL and protrudes laterally | 22 | 14.8 | 5.3 | 6.3 | 10.4 | 15 | 18.1 | 27 |
| PB overlaps PL and protrudes laterally and medially | 14 | 16.9 | 5.7 | 9.7 | 12.3 | 15.7 | 20.3 | 29 |
| PB overlaps PL and protrudes medially | 161 | 13.8 | 4.4 | 5.2 | 11.2 | 13.1 | 15.9 | 38.8 |

PB- peroneus brevis, PL- peroneus longus.

The cross-sectional area of the peroneus brevis tendon differed significantly between localisation groups (ANOVA, $p = 0.0088$). Post-hoc pairwise comparisons (Bonferroni-adjusted t-tests) showed a significantly larger area in peroneus brevis overlapping and protruding medially compared to those located medial to the peroneus longus ($p = 0.032$; Figure 7). No other pairwise differences reached statistical significance.

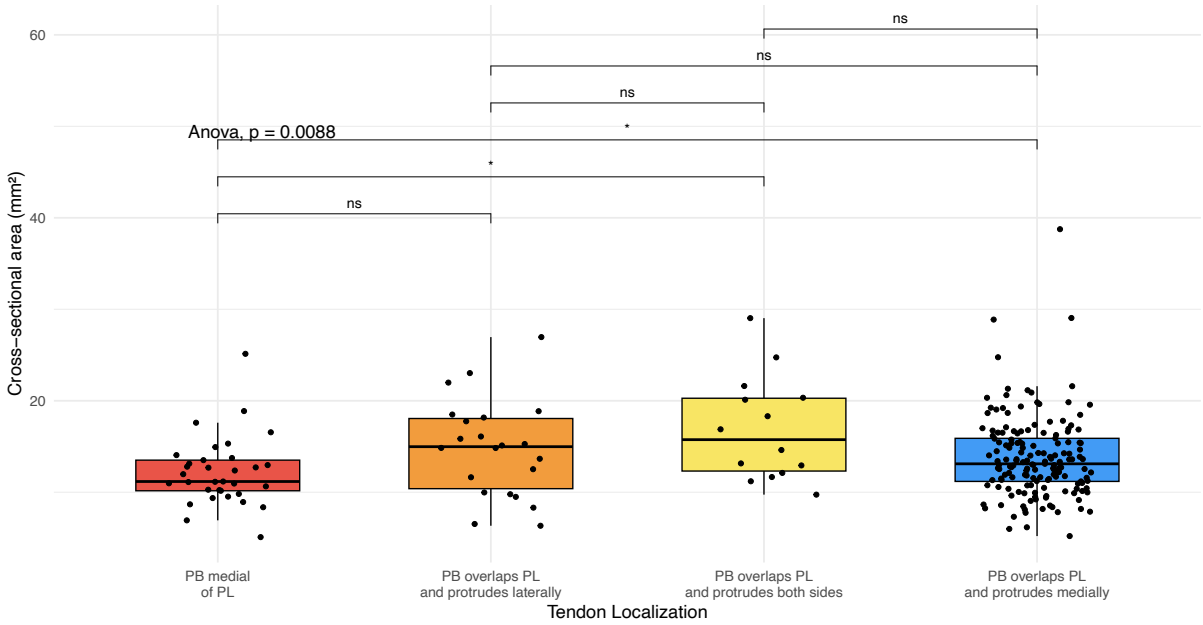


**Figure 7.** Peroneus brevis cross section area by tendon localisation, boxplot showing. Coloured boxes indicate localisation categories, and individual data points are overlaid with jitter. An overall group difference was detected using one-way analysis of variance (ANOVA) ($p = 0.0088$). Pairwise comparisons were assessed using Bonferroni-adjusted t-tests. Significant differences are marked with asterisks; non-significant comparisons are labelled 'ns'. PB – peroneus brevis, PL – peroneus longus.

## 2.6. The relationship between tendon shape and cross-sectional area

The highest mean cross-sectional area of the peroneus brevis tendon was observed in tendons with a flattened convex lateral shape (mean ± SD: 16.5 ± 6.3 mm²; Table 2).

A one-way ANOVA revealed a statistically significant differences in cross-sectional area between tendon shape categories ($F(3, 226) = 8.73$, $p < 0.001$). A post-hoc Tukey's test showed that oval-shaped tendons had a significantly smallest cross-sectional area (Figure 8).

**Table 2.** The relationship between peroneus brevis shape and cross-sectional area (in $mm^2$).

| Shape | Count | Mean | SD | Min | Q1 | Median | Q3 | Max |
|---|---|---|---|---|---|---|---|---|
| Flattened convex laterally | 25 | 16.5 | 6.3 | 6.5 | 12 | 15.1 | 21.6 | 29 |
| Flattened convex medially | 81 | 14.6 | 4.8 | 7.8 | 11.7 | 13.9 | 16.5 | 38.8 |
| General flat | 82 | 13.6 | 3.8 | 6.3 | 10.6 | 12.9 | 16.2 | 29 |
| Oval | 42 | 11.3 | 3.1 | 5.1 | 9.4 | 11.4 | 13.1 | 17.6 |

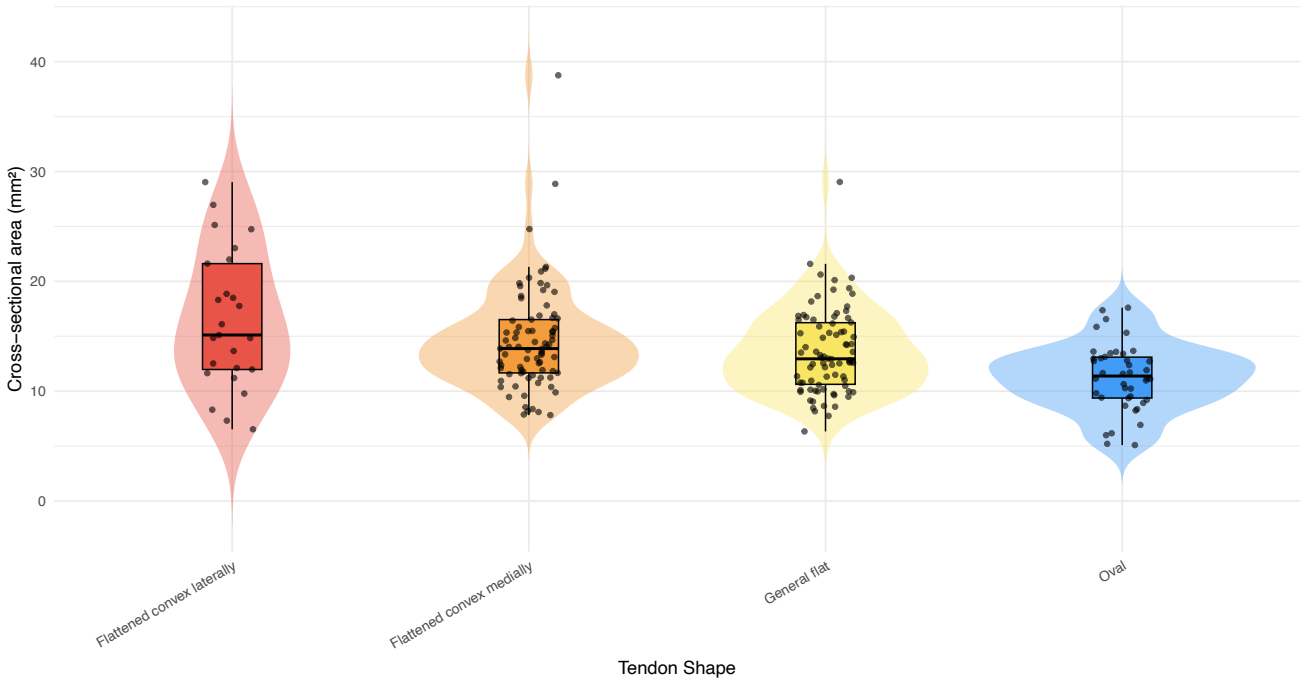


**Figure 8.** Violin plot showing the distribution of peroneus brevis tendon cross-sectional area across different tendon shapes. Boxplots indicate median and interquartile range. Jittered dots represent individual tendons.

## 2.7. Grade of the overlap between tendons

The degree of overlap between the peroneus brevis and longus tendons differed significantly across the relative localisation groups of the peroneus brevis, as shown by Fisher's exact test ($p < 0.001$), one-way ANOVA ($F(3, 226) = 46.96$, $p < 0.001$), and the Kruskal–Wallis test ($\chi^2 = 91.2$, $p < 0.001$).

The greatest overlap occurred where the peroneus brevis overlapped the longus and protruded laterally (mean ± SD: 3.2 ± 0.9 mm) and both laterally and medially (3.1 ± 0.7 mm). Almost no overlap was observed when the peroneus brevis was located medial to the longus (0.6 ± 0.6 mm; Table 3).

Post hoc analysis (Tukey HSD) showed statistically significant differences between all groups, except between the two configurations with the greatest overlap (Table 3, Figure 9).

**Table 3.** Degree of overlap (in mm) between the peroneus brevis and longus tendons across different relative tendon positions. Values are presented as mean ± standard deviation (SD).

| Relative Position | Count | Mean | SD | Mean ± SD |
|---|---|---|---|---|
| PB medial of PL | 33 | 0.6 | 0.6 | 0.6 ± 0.6 |
| PB overlaps PL and protrudes laterally | 22 | 3.2 | 0.9 | 3.2 ± 0.9 |
| PB overlaps PL and protrudes laterally and medially | 14 | 3.1 | 0.7 | 3.1 ± 0.7 |

| | | | | |
|---|---|---|---|---|
| PB overlaps PL and protrudes medially | 161 | 1.6 | 1 | 1.6 ± 1 |

PB – peroneus brevis, PL – peroneus longus.

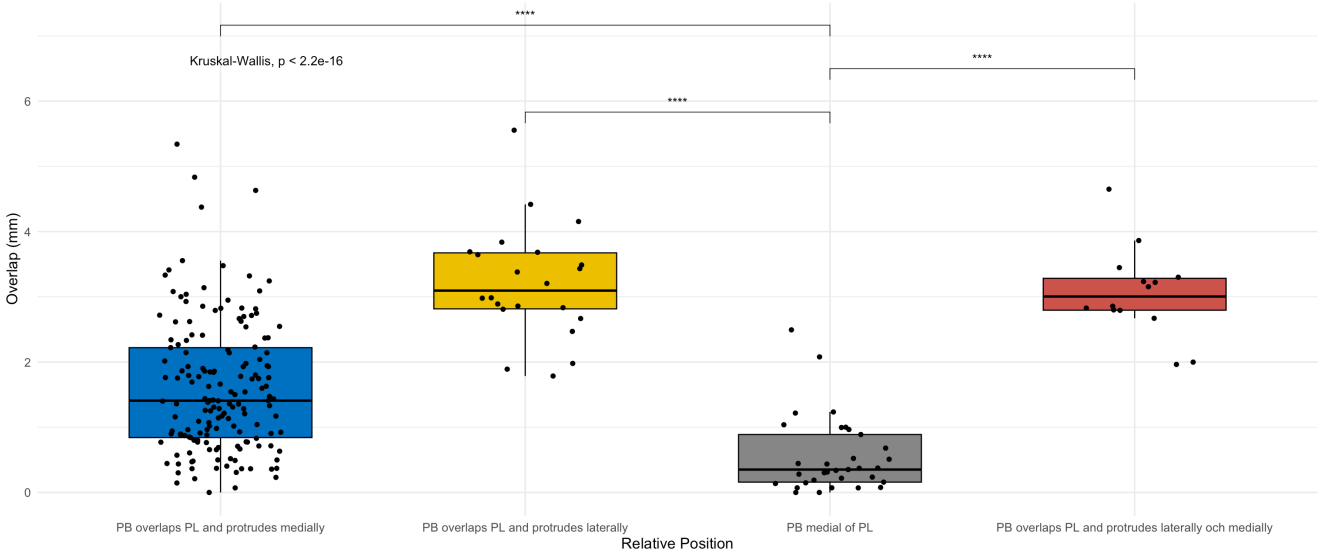


**Figure 9.** Overlap in mm across tendon positions. Boxplots display the distribution of measured overlap between the peroneus brevis and peroneus longus tendons across four anatomical positions. A Kruskal–Wallis test showed a significant overall difference ($p < 2.2\times10^{-16}$), and post hoc pairwise Wilcoxon tests (Benjamini–Hochberg adjusted) confirmed significantly greater overlap in all overlapping variants compared to the medial position (**** = $p < 0.0001$).

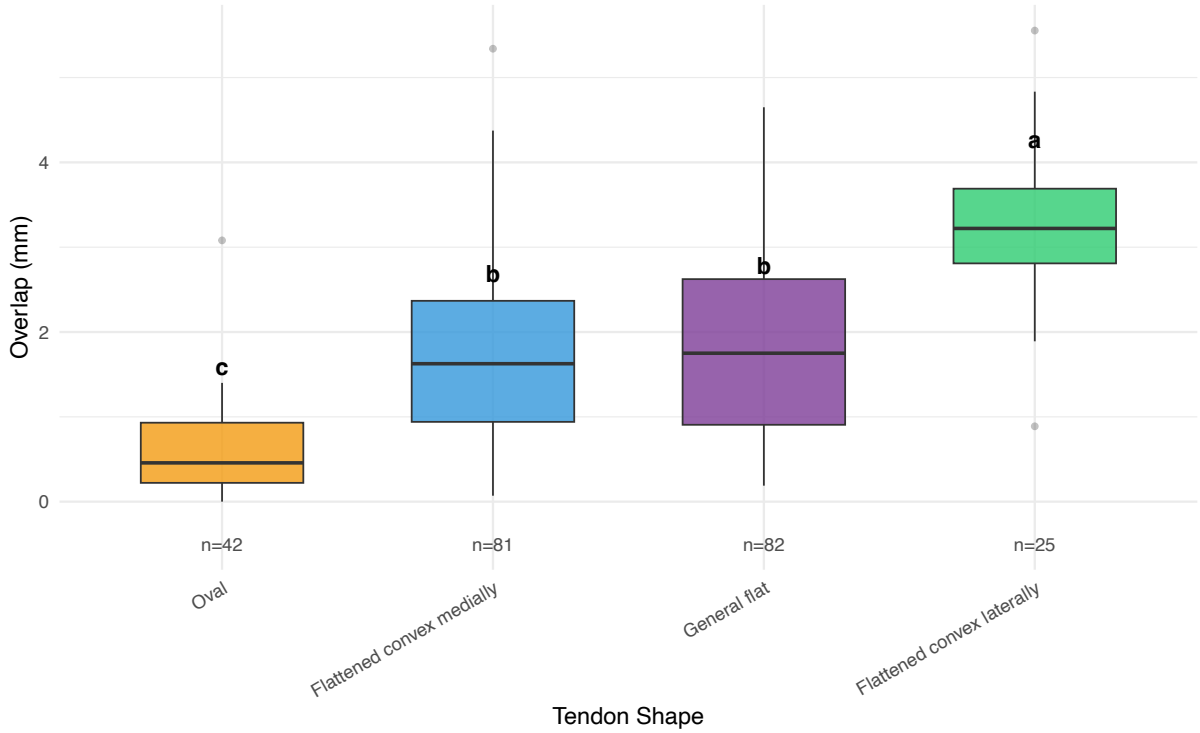


**Figure 10.** Overlap (in mm) between the peroneus brevis and longus tendons across different tendon shapes. Each boxplot shows the distribution of overlap values within each shape group, including the median, interquartile range, and outliers. Letters above the boxes indicate statistically significant groupings based on Tukey's HSD post-hoc analysis ($p < 0.05$): Groups that share the same letter were not significantly different, while groups with different letters differed significantly. The sample size for each shape group is displayed below the x-axis.

Greater tendon width (6.80 mm vs 5.48 mm, $p < 0.001$) was strongly associated with increased overlap between the peroneus tendons. Width showed the strongest correlation with overlap ($r = 0.79$), followed by area ($r = 0.35$), and thickness ($r = 0.22$) (all $p < 0.001$; Table 4, Figure 11).

**Table 4.** Pearson correlation between peroneus brevis tendon dimensions (cross-sectional area, width, and thickness) and overlap with the peroneus longus tendon.

| Variable | Pearson (r) | 95% CI lower | 95% CI upper | p value |
|---|---|---|---|---|
| PB Area vs Overlap | 0.35 | 0.23 | 0.46 | < 0.001 |
| PB Width vs Overlap | 0.79 | 0.74 | 0.83 | < 0.001 |
| PB Thickness vs Overlap | 0.22 | 0.10 | 0.34 | < 0.001 |

PB – peroneus brevis, PL – peroneus longus.

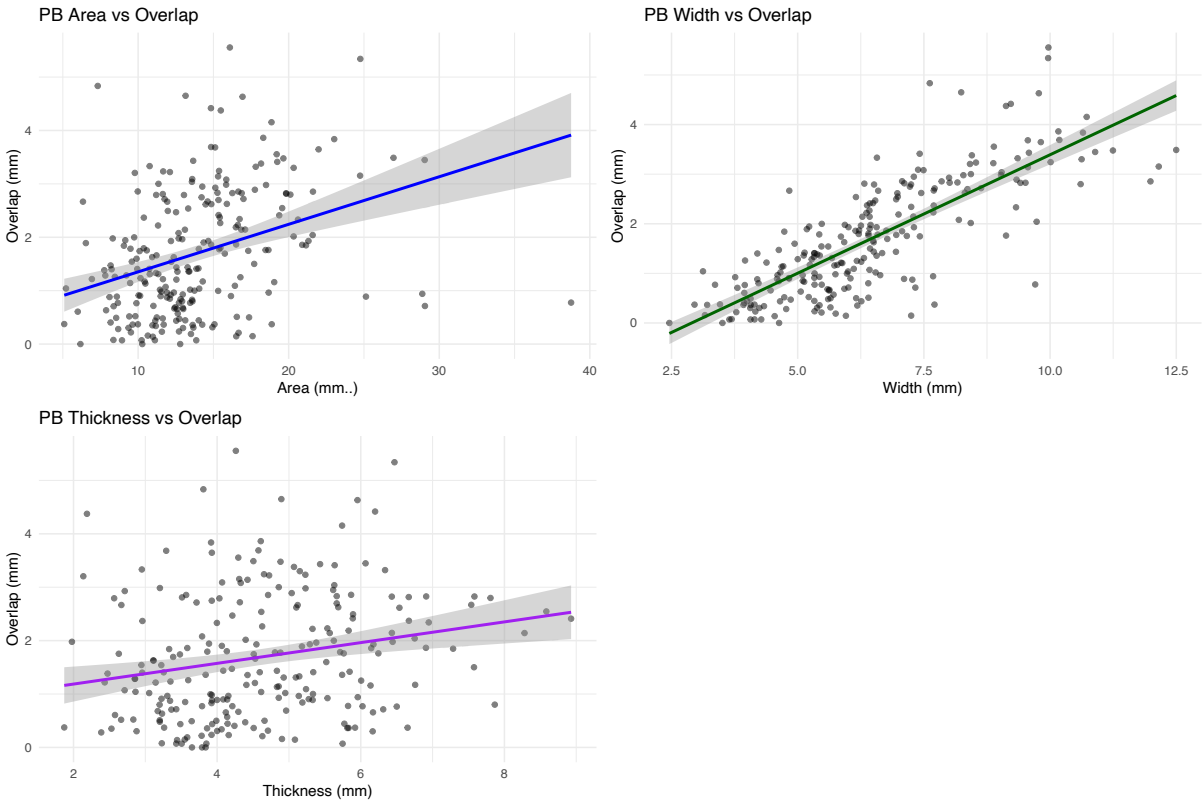


**Figure 11.** The relationship between the peroneus brevis tendon overlap and its cross-sectional area, thickness, and width. (A) Cross-sectional area, (B) width, and (C) thickness of

the peroneus brevis tendon are plotted against the measured overlap in millimetres. Each dot represents a single patient, and the blue line indicates the linear regression fit with a 95% confidence interval (CI). Width showed the strongest correlation with overlap (r = 0.79), followed by area (r = 0.35) and thickness (r = 0.22). PB – peroneus brevis.

## 2.8. Presence of low-lying peroneus brevis muscle belly

LLMB was most frequently observed in tendons overlapping the peroneus longus and protruding medially, with 60 of 161 cases (37%) demonstrating a low-lying muscle belly in this configuration. The presence of a low-lying muscle belly (LLMB) differed across peroneus brevis tendon localisations, but this variation did not reach statistical significance ($\chi^2(3) = 6.17$, $p = 0.105$; Table 5).

**Table 5.** The presence of the low-lying peroneus brevis muscle belly.

| Relative position | No | Yes | Total |
|---|---|---|---|
| PB medial of PL | 26 | 7 | 33 |
| PB overlaps PL and protrudes laterally | 18 | 4 | 22 |
| PB overlaps PL and protrudes laterally and medially | 8 | 6 | 14 |
| PB overlaps PL and protrudes medially | 101 | 60 | 161 |
| Total | 153 | 77 | 230 |

PB – peroneus brevis, PL – peroneus longus.

## 2.9. The presence of peroneus quartus

The peroneus quartus was observed in 18.3% of cases (Table 6). Fisher's exact test revealed a significant association between the presence of the peroneus quartus and the relative localisation of the peroneus brevis tendon ($p = 0.0124$).

**Table 6.** Relative position of peroneus brevis and longus in relation to peroneus quartus.

| Relative position of the peroneal tendons | Absence (n) | Absence (%) | Presence (n) | Presence (%) |
|---|---|---|---|---|
| PB medial of PL | 22 | 9.6% | 11 | 4.8% |
| PB overlaps PL and protrudes laterally | 16 | 7.0% | 6 | 2.6% |
| PB overlaps PL and protrudes laterally and medially | 10 | 4.3% | 4 | 1.7% |
| PB overlaps PL and protrudes medially | 140 | 60.9% | 21 | 9.1% |
| Total | 188 | 81.7% | 42 | 18.3% |

PB – peroneus brevis, PL – peroneus longus.

The highest percentages of the presence of the peroneus quartus were in the general flat and flattened convex laterally tendons (Table 7). Both the Chi-square test ($X^2 = 6.00$, $p = 0.1114$) and Fisher's Exact Test ($p = 0.1051$) suggest that there is no significant association between the shape of the peroneus brevis and the presence of the peroneus quartus.

**Table 7.** The shape of the peroneus brevis on the cross-sectional area vs the presence of the peroneus quartus.

| Shape of Peroneus Brevis | Absence (n) | Absence (%) | Presence (n) | Presence (%) |
|---|---|---|---|---|
| Flattened convex laterally | 17 | 7.4% | 8 | 3.5% |
| Flattened convex medially | 71 | 30.9% | 10 | 4.3% |
| General flat | 68 | 29.6% | 14 | 6.1% |
| Oval | 32 | 13.9% | 10 | 4.3% |
| Total | 188 | 81.7% | 42 | 18.3% |

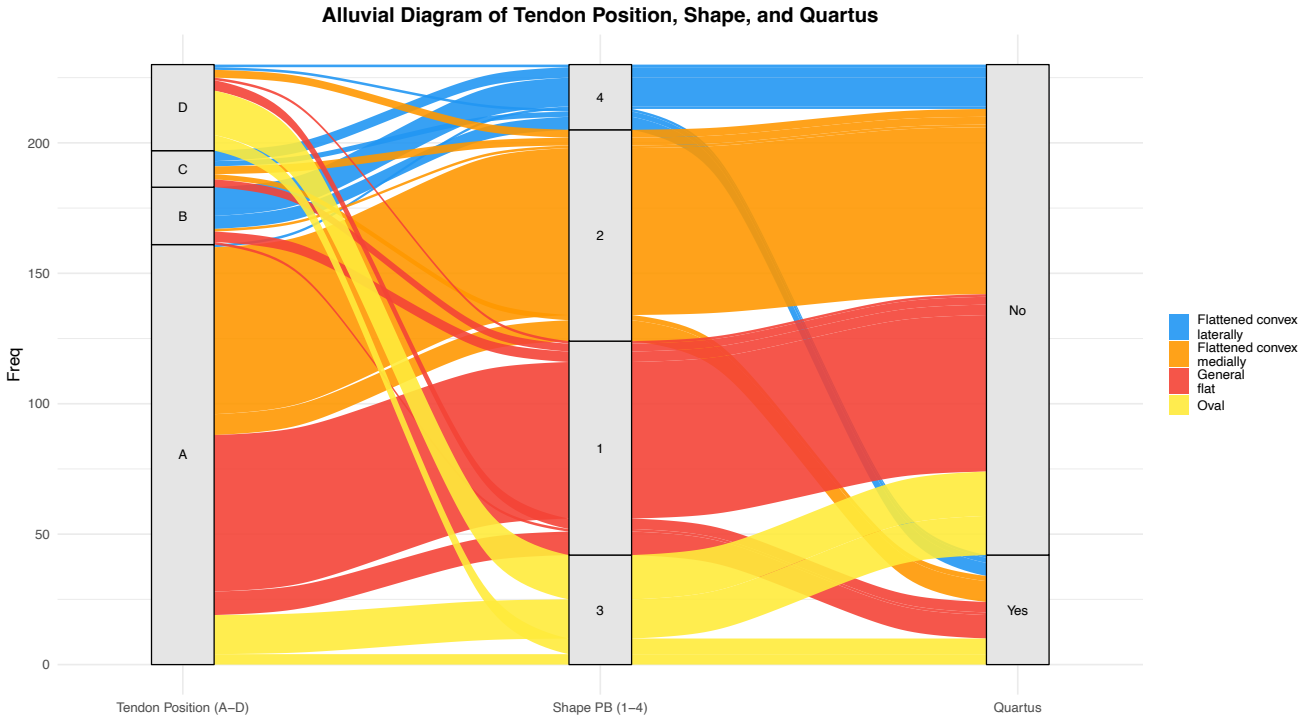


**Figure 12.** The alluvial diagram shows the relationship between the peroneus brevis (PB) position, the shape of the tendons on the transverse cross-section, and the presence of the peroneus quartus. Peroneus brevis positions are labelled A to D: A – PB overlaps the peroneus longus (PL) and protrudes medially, B – PB protrudes laterally, C – PB protrudes both laterally and medially, and D – PB is medial to PL. The PB shape is classified into four groups: 1– general flat, 2 – flattened convex medially, 3 – oval, and 4 – flattened convex laterally. Presence and absence of the peroneus quartus are marked as yes or no. The width of the links in the diagram indicates the distribution of tendons in each category.

## 2.10. Modelling of tendon position

A multiple linear regression model was used to assess the association between variables and the peroneal tendons overlap in mm. Seventeen influential observations were excluded based on Cook's distance (threshold: 4/n). The final model included four predictors: the presence of the peroneus quartus muscle, the presence of a low-lying muscle belly, the cross-sectional area of the peroneus longus, and the width of the peroneus brevis (Table 8, Figure 13). The presence of the peroneus quartus was significantly associated with increased tendon overlap ($\beta = 0.22$ mm, 95% CI: 0.02–0.42, $p = 0.03$). Although predicted values suggested a steeper increase in overlap among individuals with both a peroneus quartus and a low-lying muscle belly (Figure 14), the latter did not reach statistical significance in the multivariable model ($p = 0.17$). The overlap increased substantially with peroneus brevis width ($\beta = 0.51$ mm per mm, 95% CI: 0.47–0.55, $p < 0.001$) and decreased slightly with greater peroneus longus area ($\beta = -0.03$ mm per mm², 95% CI: -0.04 to -0.01, $p < 0.001$).

Details on multicollinearity, influential observations, and robustness analyses (including standardised coefficients and bootstrapped confidence intervals) are available in the appendix (Tables S1–S5).

**Table 8.** Linear regression model evaluating predictors of peroneal tendon overlap (in millimetres) after exclusion of influential observations. Estimates represent unstandardised regression coefficients.

| Term | Estimate | Std error | Statistic | p value | conf low | conf high |
|---|---|---|---|---|---|---|
| (Intercept) | -1.15 | 0.18 | -6.46 | 0.00 | -1.51 | -0.80 |
| Peroneus quartus | 0.22 | 0.10 | 2.13 | 0.03 | 0.02 | 0.42 |

| | | | | | | |
|---|---|---|---|---|---|---|
| Low-lying muscle belly of peroneus brevis | 0.11 | 0.08 | 1.39 | 0.17 | -0.05 | 0.27 |
| Peroneus longus cross section area in mm2 | -0.03 | 0.01 | -3.86 | 0.00 | -0.04 | -0.01 |
| Width of the peroneus brevis tendon in mm | 0.51 | 0.02 | 23.54 | 0.00 | 0.47 | 0.55 |

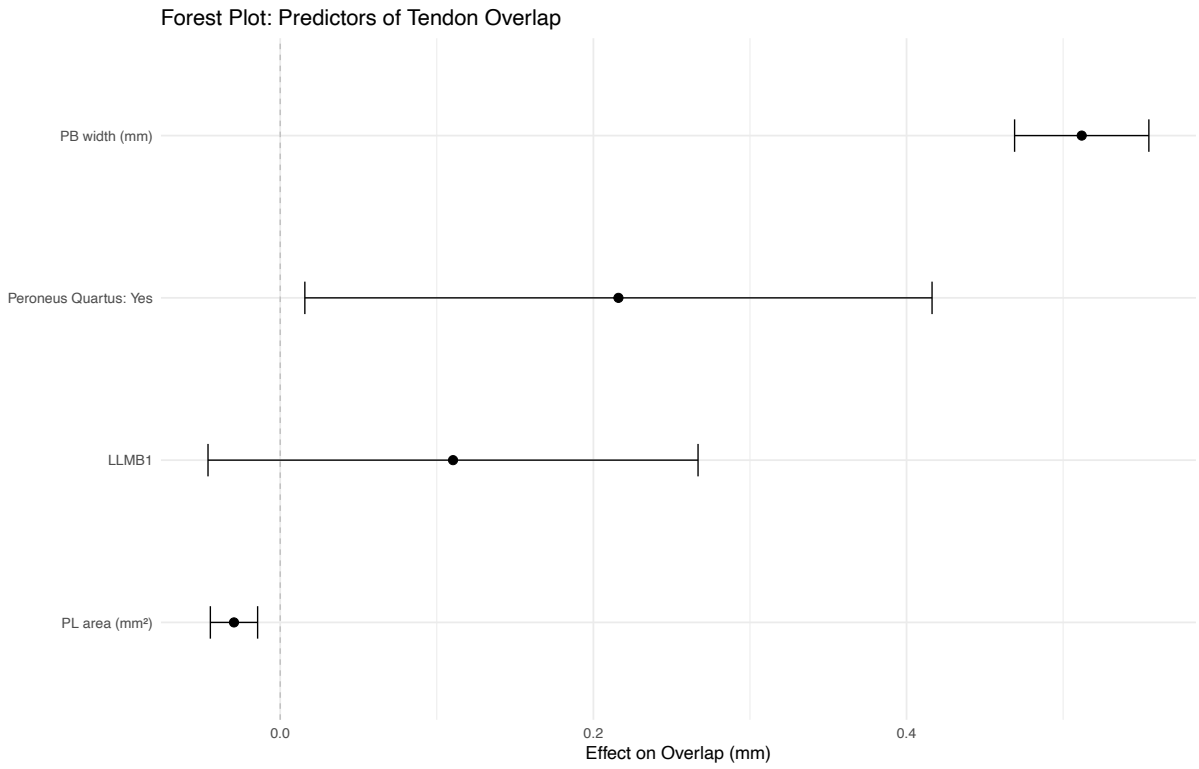


**Figure 13.** Forest plot showing effect sizes and 95% confidence intervals for predictors of tendon overlap. Peroneus brevis width had the strongest association, followed by peroneus longus area and presence of a peroneus quartus. LLMB1- presence of low-lying muscle belly of peroneus brevis. PB- peroneus brevis, PL- peroneus longus.

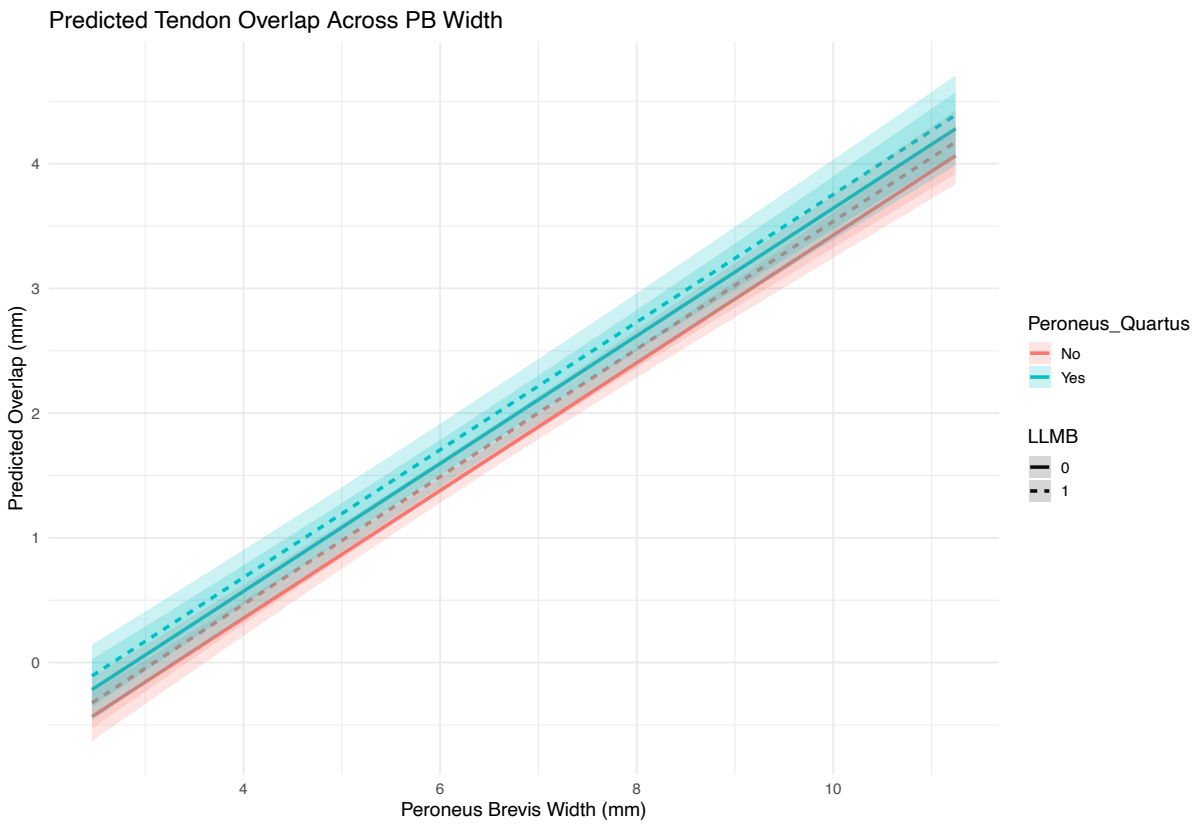


**Figure 14.** Predicted tendon overlap (mm) across the range of peroneus brevis widths, stratified by presence of a peroneus quartus and a low-lying muscle belly. Overlap increased consistently with width, with the steepest slope observed in cases with both anatomical variants. LLMB1- presence of low-lying muscle belly of peroneus brevis. PB- peroneus brevis.

## Discussion

To the best of our knowledge, this is the first study to systematically assess anatomical variation in the position of the peroneus brevis tendon and factors that impact it in a large in vivo population with MRI. Our study demonstrates that the position and morphology of the peroneus brevis tendon exhibit substantial anatomical variation. In the most common configuration, the peroneus brevis overlaps the peroneus longus and protrudes medially, yet other variants were identified. Tendon shape was closely related to its position: medially positioned tendons were typically oval-shaped, while overlapping tendons, particularly those protruding laterally, were more often flattened and wider. Flattened tendons also had a larger cross-sectional area, indicating that tendon shape and size are strongly interconnected. Furthermore, the presence of the peroneus quartus muscle was most often seen in tendons with lateral or combined protrusions, especially those with a laterally convex shape. These interrelated anatomical features point to a structured, rather than random, variation in tendon morphology. Understanding these patterns is clinically important. Variants in position and shape may influence imaging interpretation. We noticed that tendons that protrude laterally in asymptomatic individuals may, in our opinion, be misinterpreted as instability since the peroneus brevis tend to be more lateral in relation to the peroneus longus. Interpreting this variant as pathology may lead to unnecessary surgery. To better understand relationships between localisation, we performed multivariate regression analysis to quantify the impact of specific anatomical features on tendon positioning.

Tendon shape emerged as a key determinant of tendons' localisation. Oval-shaped tendons were most frequently located medial to the peroneus longus, while flattened tendons, particularly those with lateral convexity, were more likely to overlap the longus tendon and protrude laterally or in both directions. The shape of the peroneus brevis tendon may be

related to the occurrence of longitudinal split tears, according to some authors [9]. The localisation between the peroneal tendons is particularly relevant in the context of tendon instability assessment and the possible risk of the split tear. Moreover, the cross-sectional area of the tendon was related to its shape, with flattened convex medially having the largest area. Flattened tendons, particularly those with lateral convexity, exhibited the largest cross-sectional areas, while oval tendons had the smallest. During dorsiflexion, the peroneus brevis tendon becomes more flattened and compressed against the fibular groove by the overlying peroneus longus tendon. This observation from the previous studies is true if the tendons are related in the most common variant. But if the peroneus brevis is located medially, this theory is not valid. However, there are no studies regarding which anatomical shape is more related to the split. Pathomechanics for longitudinal splitting is not known; some studies suggest tendon shape as a potentially important factor in the pathogenesis of split tears [15]. Tendons positioned in overlapping configurations had significantly greater width and thickness, indicating that bulkier tendons are more likely to deviate from a colinear arrangement with the peroneus longus. It can be hypothesised that increased tendon cross-sectional area may mechanically drive or accommodate changes in position.

The significance of the change in shape can be illustrated by a pathological finding, which was a peroneus brevis encircling the peroneus longus. This configuration can mimic the so-called boomerang sign on MRI, which has been associated with peroneal tendinopathy and may indicate an underlying split tear. However, this anatomical variant showed no signal abnormalities on T2- or PD-weighted images and maintained central tendon continuity, distinguishing it from true split tears, which present with separated tendon fragments and interposed fluid across multiple slices [4]. Awareness of this variant is essential to prevent overdiagnosis of peroneal tendon pathology.

In a small subset of cases, we identified tendons with greater lateral thickness than medial, raising questions about whether this may represent early subclinical and sub-radiological tendinosis. However, patients with higher signal on proton density- or T2-weighted images were excluded, and no signal abnormalities were detected in the included tendons. While subclinical changes cannot be ruled out entirely, conventional MRI lacks sensitivity for early-stage degenerative processes. Advanced techniques such as T2-mapping [22], ultrashort echo time (UTE) MRI may improve detection of such changes [5], as they allow imaging of tissues with very short T2 relaxation times that are not visible on conventional sequences [24]. However, there are no studies on the peroneal tendons. Still, in the absence of signal changes, these shape variants are more likely to represent anatomical variation than pathology. However, further studies are needed to evaluate this. Some age-related tendon changes were noticed. Older individuals had larger peroneus brevis cross-sectional areas than younger patients, yet no signal abnormalities or changes in tendon morphology were observed and were interpreted carefully. This likely reflects physiological ageing rather than pathology, which can now be detected with diagnostic methods. Recognising these normal variations is particularly important in ageing populations, where imaging findings may be misinterpreted as signs of tendinosis or tear.

A multiple linear regression model confirmed that the presence of a peroneus quartus muscle and the width of the peroneus brevis tendon were independently associated with increased tendon overlap. Overlap also increased with a smaller peroneus longus area, while the low-lying muscle belly showed no independent effect. Notably, the predicted values suggested steeper increases in overlap among individuals with both anatomical variants, but only the peroneus quartus reached statistical significance. The dynamic balance between the components of the superior peroneal tunnel may be an important factor influencing the position of the peroneus brevis tendon. Findings from our study indicate that the peroneus

brevis tendon position is variable and related to anatomical factors, such as its own morphology, peroneus longus, the presence of peroneus quartus and low-lying muscle belly. These variations should be recognised in clinical practice, especially in the evaluation of peroneal instability, pre-surgical planning, and in distinguishing anatomical variants from pathology. It is particularly important for radiologists reporting ankle MRI not to take the normal finding as pathology.

Anatomical variations may also modify the relationship between structures. We found a significant association between the presence of the peroneus quartus muscle and certain positional and morphological features. The peroneus quartus was most frequently observed in cases where the peroneus brevis tendon protruded laterally or medially, particularly when the tendon displayed lateral convexity. This suggests that accessory musculature may contribute to changes in tendon trajectory during flexion, possibly through altered biomechanics or competition for space in the superior peroneal tunnel. However, due to the limited number of quartus-positive cases, these associations should be interpreted cautiously and further studies are needed.

Our study has several limitations, including its retrospective design, lack of histological correlation, and single-centre setting. Future studies incorporating multicentre data and histological validation could provide further insights into the clinical significance of these anatomical variations.

## Conclusion

The localisation of the peroneus brevis tendon varies substantially, with the most common configuration involving overlap with the peroneus longus and medial protrusion. Other consistent patterns—such as medial, lateral, and combined protrusions—were also observed.

These positional variants were closely linked to tendon morphology: oval tendons were typically positioned medial to the peroneus longus, while flattened tendons were more often found in overlapping configurations. Wider and thicker tendons were more likely to deviate from a colinear position and overlap the longus tendon. The peroneus quartus muscle was most frequently associated with tendons that overlapped and protruded medially. Regression analysis confirmed that peroneus brevis width and the presence of a peroneus quartus muscle were independently associated with increased tendon overlap, providing quantitative support for these anatomical relationships.

Understanding this anatomical variability is clinically important. Positional and morphological variants are normal findings, yet they may influence the imaging appearance of the peroneal tendons and should not be mistaken for pathology. These observations highlight the importance of recognising anatomical patterns and raise important questions about whether certain configurations may predispose to instability or splitting. Future studies should investigate the clinical relevance of these variants, particularly their potential association with split tears.

## Declarations

**Declaration of Generative AI and AI-assisted technologies in the writing process**

Nothing to disclose

**Ethics approval and consent to participate**

All procedures performed in studies involving human participants were in accordance with the ethical standards of the institutional and/or national research committee and with the 1964

Helsinki Declaration and its later amendments or comparable ethical standards. The Swedish Ethical Authority approved this study and waived informed consent (number 2024-07283-02).

**Consent for publication**

Not applicable. The manuscript does not contain the data of individuals in any form.

**Availability of data and material**

Yes

**Competing interests**

The authors declare that they have no competing interests.

**Funding**

This work was supported by Stiftelsen Tornspiran (934: 2023-12-01) and by the Swedish state under the agreement between the Swedish Government and the county councils, the ALF-agreement (ALFGBG-1006741).

**Authors' contributions**

Conceptualization: PS; Methodology: PS, KBD, RZ; Software: PS, RZ; Data Collection: All authors; Data Curation: RZ, PS; Writing – Original Draft: RZ, PS; Writing – Review and Editing: All authors. All authors contributed to previous manuscript versions, and all have read and approved the final manuscript.

**Acknowledgements**

None

## References

1. Bokwa-Dabrowska K, Mocanu D, Alexiev A, et al (2024) Peroneus brevis split rupture is underreported on magnetic resonance imaging of the ankle in patients with chronic lateral ankle pain. Eur J Radiol Open 13:100591. https://doi.org/10.1016/j.ejro.2024.100591.
2. Davda K, Malhotra K, O'Donnell P, et al (2017) Peroneal tendon disorders. EFORT Open Rev 2:281-292. https://doi.org/10.1302/2058-5241.2.160047.
3. Galli MM, Protzman NM, Mandelker EM, et al (2015) An examination of anatomic variants and incidental peroneal tendon pathologic features: a comprehensive MRI review of asymptomatic lateral ankles. J Foot Ankle Surg 54:164-172. https://doi.org/10.1053/j.jfas.2014.11.005.
4. Gorelik N, Boily M, Lafreniere AS, et al (2020) Impact of the T2-weighted axial oblique MRI sequence in the assessment of peroneal tendons. Clin Radiol 75:642 e615-642 e623. https://doi.org/10.1016/j.crad.2020.02.018.
5. Hodgson RJ, O'Connor PJ, Grainger AJ (2012) Tendon and ligament imaging. Br J Radiol 85:1157-1172. https://doi.org/10.1259/bjr/34786470.
6. Housley SN, Lewis JE, Thompson DL, et al (2017) A Proximal Fibularis Brevis Muscle Is Associated with Longitudinal Split Tendons: A Cadaveric Study. J Foot Ankle Surg 56:34-36. https://doi.org/10.1053/j.jfas.2016.09.009.
7. Kuwada GT (2008) Surgical correlation of preoperative MRI findings of trauma to tendons and ligaments of the foot and ankle. J Am Podiatr Med Assoc 98:370-373. https://doi.org/10.7547/0980370.
8. Landis JR, Koch GG (1977) The measurement of observer agreement for categorical data. Biometrics 33:159-174.
9. Major NM, Helms CA, Fritz RC, et al (2000) The MR imaging appearance of longitudinal split tears of the peroneus brevis tendon. Foot Ankle Int 21:514-519. https://doi.org/10.1177/107110070002100612.
10. Michels F, Wastyn H, Pottel H, et al (2022) The presence of persistent symptoms 12 months following a first lateral ankle sprain: A systematic review and meta-analysis. Foot Ankle Surg 28:817-826. https://doi.org/10.1016/j.fas.2021.12.002.
11. Mirmiran R, Squire C, Wassell D (2015) Prevalence and Role of a Low-Lying Peroneus Brevis Muscle Belly in Patients With Peroneal Tendon Pathologic Features: A Potential Source of Tendon Subluxation. J Foot Ankle Surg 54:872-875. https://doi.org/10.1053/j.jfas.2015.02.012.
12. Miura K, Ishibashi Y, Tsuda E, et al (2004) Split lesions of the peroneus brevis tendon in the Japanese population: an anatomic and histologic study of 112 cadaveric ankles. J Orthop Sci 9:291-295. https://doi.org/10.1007/s00776-004-0784-5.

13. Olewnik L, Podgorski M, Ruzik K, et al (2020) New classification of the distal attachment of the fibularis brevis - Anatomical variations and potential clinical implications. Foot Ankle Surg 26:308-313. https://doi.org/10.1016/j.fas.2019.04.002.
14. Olewnik L, Zielinska N, Ruzik K, et al (2024) Morphological variability of the fibularis brevis tendon in human fetuses. Ann Anat 251:152154. https://doi.org/10.1016/j.aanat.2023.152154.
15. Rademaker J, Rosenberg ZS, Delfaut EM, et al (2000) Tear of the peroneus longus tendon: MR imaging features in nine patients. Radiology 214:700-704. https://doi.org/10.1148/radiology.214.3.r00mr35700.
16. Ruzik K, Westrych K, Konschake M, et al (2022) Case report of unusual insertion of the fibularis brevis muscle. Surg Radiol Anat 44:485-489. https://doi.org/10.1007/s00276-022-02894-y.
17. Schweitzer ME, Eid ME, Deely D, et al (1997) Using MR imaging to differentiate peroneal splits from other peroneal disorders. AJR Am J Roentgenol 168:129-133. https://doi.org/10.2214/ajr.168.1.8976935.
18. Sharma A, Parekh SG (2020) Pathologies of the Peroneals: A Review. Foot Ankle Spec 1938640020916278. https://doi.org/10.1177/1938640020916278.
19. Sobel M, Bohne WH, Levy ME (1990) Longitudinal attrition of the peroneus brevis tendon in the fibular groove: an anatomic study. Foot Ankle 11:124-128. https://doi.org/10.1177/107110079001100302.
20. Sobel M, Geppert MJ, Warren RF (1993) Chronic ankle instability as a cause of peroneal tendon injury. Clin Orthop Relat Res 187-191.
21. Squires N, Myerson MS, Gamba C (2007) Surgical treatment of peroneal tendon tears. Foot Ankle Clin 12:675-695, vii. https://doi.org/10.1016/j.fcl.2007.08.002.
22. Stein P, Wuennemann F, Schneider T, et al (2023) Detection and Quantitative Assessment of Arthroscopically Proven Long Biceps Tendon Pathologies Using T2 Mapping. Tomography 9:1577-1591. https://doi.org/10.3390/tomography9050126.
23. Taljanovic MS, Alcala JN, Gimber LH, et al (2015) High-resolution US and MR imaging of peroneal tendon injuries. Radiographics 35:179-199. https://doi.org/10.1148/rg.351130062.
24. Tyler DJ, Robson MD, Henkelman RM, et al (2007) Magnetic resonance imaging with ultrashort TE (UTE) PULSE sequences: technical considerations. J Magn Reson Imaging 25:279-289. https://doi.org/10.1002/jmri.20851.
25. Unlu MC, Bilgili M, Akgun I, et al (2010) Abnormal proximal musculotendinous junction of the peroneus brevis muscle as a cause of peroneus brevis tendon tears: a cadaveric study. J Foot Ankle Surg 49:537-540. https://doi.org/10.1053/j.jfas.2010.09.001.
26. van Dijk PA, Miller D, Calder J, et al (2018) The ESSKA-AFAS international consensus statement on peroneal tendon pathologies. Knee Surg Sports Traumatol Arthrosc 26:3096-3107. https://doi.org/10.1007/s00167-018-4971-x.
27. von Elm E, Altman DG, Egger M, et al (2007) The Strengthening the Reporting of Observational Studies in Epidemiology (STROBE) statement: guidelines for reporting observational studies. Lancet 370:1453-1457. https://doi.org/10.1016/S0140-6736(07)61602-X.
28. Wang XT, Rosenberg ZS, Mechlin MB, et al (2005) Normal variants and diseases of the peroneal tendons and superior peroneal retinaculum: MR imaging features. Radiographics 25:587-602. https://doi.org/10.1148/rg.253045123.
29. Zielinska N, Tubbs RS, Gonera B, et al (2024) The tendon of the fibularis brevis muscle - Systematic overview and new classification system. Ann Anat 253:152208. https://doi.org/10.1016/j.aanat.2023.152208.